Appl. Phys. B 84, 471–478 (2006)
DOI: 10.1007/s00340-006-2287-x

Applied Physics B
Lasers and Optics

MAHMOUD ABDEL-ATY

Generation of long-living entanglement using cold trapped ions with pair cat states

[1] Mathematics Department, Faculty of Science, South Valley University, 82524, Sohag, Egypt
[2] Mathematics Department, College of Science, Bahrain University, 32038, Kingdom of Bahrain

Received: 21 January 2006/Final version: 23 April 2006
Published online: 23 June 2006 •

ABSTRACT With the reliance in the processing of quantum information on a cold trapped ion, we analyze the entanglement entropy in the ion-field interaction with pair cat states. We investigate a long-living entanglement allowing the instantaneous position of the center-of-mass motion of the ion to be explicitly time-dependent. An analytic solution for the system operators is obtained. We show that different nonclassical effects arise in the dynamics of the population inversion, depending on the initial states of the vibrational motion. We study in detail the entanglement degree and demonstrate how the input pair cat state is required for initiating the long-living entanglement. This long-living entanglement is damp out with an increase in the number difference q. Owing to the properties of entanglement measures, the results are checked using another entanglement measure (high order linear entropy).

PACS 03.67.Nm; 03.65.Yz; 42.50.Dv

1 Introduction

Recent advances in the dynamics of trapped ions (for a recent review, see e.g., [1]) have demonstrated that a macroscopic observer can effectively control dynamics as well as perform a complete measurement of states of microscopic quantum systems. By coupling the electronic and vibrational states of a trapped ion with laser radiation, motional wavepackets of the ion can be manipulated and interesting states of motion, such as Fock states, squeezed states or Schrödinger-cat states, can be created which exhibit highly nonclassical behavior [2, 3]. In order to observe these nonclassical features, methods for trapped ion quantum state tomo graphy have been proposed [4, 5]. Experimental preparation and measurement of the the motional state of a trapped ion, which has been initially laser cooled to the zero-point of motion, has been reported in [6].

On the other hand, the characterization of entangled states and entanglement is a challenging problem and considerable theoretical efforts have been invested in characterizing entang lement in a variety of physical situations [7–11]. Creation and characterization of entangled states of up to eight trapped ions, the investigation of long-lived two-ion Bell-states, and experiments towards entangling ions have recently been reported [12].

The main motivation for the present work is twofold: first, we demonstrate how a pair cat state affects the entanglement for the ion-field interaction, and second to see how the time-dependent amplitude of the irradiating laser field affect this entanglement. In particular, we consider a single trapped ion which can be laser cooled to the ground state of the trapping potential and discuss the roles played by the initial state setting and time-dependent amplitude of the laser field on the entanglement.

The paper is presented as follows: Sect. 2 is devoted to a brief description of the pair cat state and the relation of the quadrature distribution to the entanglement. In Sect. 3, we present the quantized model and obtain an exact analytical solution of the system operators. In Sect. 4, we briefly discuss the atomic inversion related to the collapse-revival phenomena. In Sect. 5, we analyze in detail how the pair cat state affect the general features of von Neumann entropy (a measure of the ion-field entanglement). This gives us the opportunity to stress the essential role played by pair cat states in this context and study the existing of a long living entanglement. We summarize our results at the end of the paper and make some conclusions.

2 Pair cat states

In the well-known cat paradox, Schrödinger tried to demonstrate a possibility of generating a quantum superposition of a macroscopic system [13]. Superpositions of orthogonal states which exhibits macroscopic features appear to be of fundamental importance in recent studies of the foundations of quantum mechanics.

In terms of conventional coherent states parameterized in terms of a complex number α [14, 15], the Schrödinger cat state has the following form

$$|S_{\rm cat}\rangle \equiv \frac{1}{\sqrt{2+2\cos\varphi\exp(-|\alpha|^2)}}\left(|\alpha\rangle + {\rm e}^{{\rm i}\varphi}|-\alpha\rangle\right), \qquad (1)$$

where $|\alpha\rangle$ is a coherent state of amplitude α, and φ is a real local phase factor. Note that the relative phase φ can be approximately controlled by the displacement operation for a given cat state with $\alpha \gg 1$. Schrödinger cat states of this type

✉ Fax: +973 17640862, E-mail: abdelatyquantum@yahoo.co.uk

have been realized for a trapped $^9Be^+$ ion [14]. A special set of coherent states of the Barut–Girardello type known as pair coherent states has been formulated [16]. If $\widehat{a}^\dagger(\widehat{a})$ and $\widehat{b}^\dagger(\widehat{b})$ denote two independent boson creation (annihilation) operators, then $\widehat{a}\widehat{b}(\widehat{a}^\dagger\widehat{b}^\dagger)$ stands for the pair annihilation (creation) operator for the two modes. The pair coherent states $|\xi, q\rangle$ are defined as eigenstates of both the pair annihilation operator $\widehat{a}\widehat{b}$ and the number difference operator $\widehat{a}^\dagger\widehat{a}-\widehat{b}^\dagger\widehat{b}$, i.e.,

$$\widehat{a}\widehat{b}|\xi, q\rangle \equiv \xi|\xi, q\rangle\,, \qquad \left(\widehat{a}^\dagger\widehat{a}-\widehat{b}^\dagger\widehat{b}\right)|\xi, q\rangle = q|\xi, q\rangle \tag{2}$$

where ξ is a complex number and q is the charge parameter, which is a fixed integer. Furthermore, the pair coherent states can be expanded as a superposition of the two-mode Fock states,

$$|\xi, q\rangle \equiv N_q \sum_{n=0}^{\infty} \frac{\xi^n}{\sqrt{n!(n+q)!}}|n, n+q\rangle\,, \tag{3}$$

where N_q is the normalization constant and can be written as $N_q = \left[|\xi|^{-q} J_q(2|\xi|)\right]^{-\frac{1}{2}}$, where J_q is the modified Bessel function of the first kind of order q. Pair coherent states are regarded as an important type of correlated two-mode state, which possess prominent nonclassical properties such as sub-Poissonian statistics, correlation in the number fluctuations, squeezing, and violations of Cauchy–Schwarz inequalities [17, 18]. The pair cat states are defined as a superposition of two pair coherent states separated in phase by 180° [19],

$$|\xi, q, \varphi\rangle \equiv N_\varphi\left(|\xi, q\rangle + \exp(\mathrm{i}\varphi)|-\xi, q\rangle\right)\,, \tag{4}$$

where the normalization factor N_φ is given by

$$N_\varphi = \frac{1}{\sqrt{2}}\left(1 + N_q^2\cos\varphi\sum_{n=0}^{\infty}\frac{(-1)^n|\xi|^{2n}}{n!(n+q)!}\right)^{-\frac{1}{2}}\,. \tag{5}$$

It has been shown that these cat states may exhibit stronger nonclassical effects than the corresponding pair coherent states. The correlated two-mode cat state $|\xi, q, \varphi\rangle$ is the eigenstate of the operators $\widehat{a}^2\widehat{b}^2$ and $\widehat{a}^\dagger\widehat{a}-\widehat{b}^\dagger\widehat{b}$ with eigenvalues ξ^2 and q, respectively. In order to generate such cat states for the motion in a two-dimensional anisotropic trap we require two laser beams. Due to the strong nonclassical nature of the two-mode cat states, the generation of such states is of interest in testing fundamental of quantum mechanics.

The coordinate space wave function is given by

$$\begin{aligned}\langle x, y|S\rangle &= N_\varphi\left(\langle x, y|\xi, q\rangle + \exp(\mathrm{i}\varphi)\,\langle x, y|-\xi, q\rangle\right)\\ &= N_\varphi\sum_{n=0}^{\infty}\left(1+(-1)^n\mathrm{e}^{\mathrm{i}\varphi}\right)\langle x|n+q\rangle\langle y|n\rangle\,,\end{aligned} \tag{6}$$

where $\langle x|n\rangle$ is a harmonic oscillator wave function. In this case, the quadrature distribution is given by

$$\begin{aligned}P(x, y) = |N_\varphi|^2\Bigg|\sum_{n=0}^{\infty}\frac{(1+(-1)^n\mathrm{e}^{\mathrm{i}\varphi})}{\pi}\frac{2^{-(2n+q)}}{n!(n+q)!}\\ \times H_{n+q}(x)H_n(y)\mathrm{e}^{-0.5(x^2+y^2)}\Bigg|^2\,.\end{aligned} \tag{7}$$

For fixed values of the parameter q the periodic nature in the quadrature distribution function for different values of the parameter ξ is shown in Fig. 1, where we plot $P(x, y)$ for $\xi = 0.1$, 1 and 3. It is shown that the regions of the quadrature distribution in the (x, y)-plane are symmetric with respect to

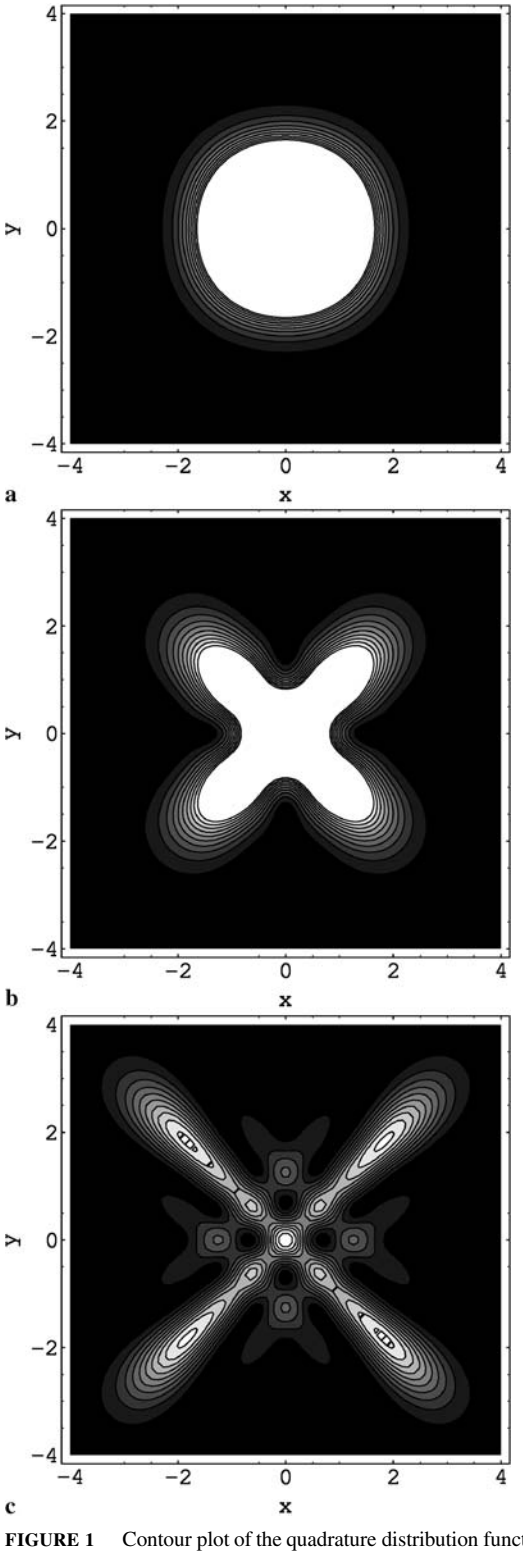

FIGURE 1 Contour plot of the quadrature distribution function $P(x, y)$ for the pair cat state for $q = 0$, $\varphi = \pi/2$ and for different values of the parameter ξ where (**a**) $\xi = 0.1$, (**b**) $\xi = 1$ and (**c**) $\xi = 3$

$y = -x$ and with respect to $y = x$ (Fig. 1b and c). It is clear that the present distribution reflects the entanglement present in the two-mode pair cat states. The main curiosity is that, if squeezing is strong enough, the ring-like quadratic distribution function collapses to a quasi one dimensional object with a cigar form (see Fig. 1a).

The origin of such behavior is in the generation of pair cat states in the microscopic regime, where the contributions of the different components of the pair cat states are located close to the phase space origin, competing with each other. For increased value of the parameter ξ, the shape of the quadrature distribution becomes more pronounced by involving multipeak structure (symmetric peaks). This is in a good agreement with the general behavior of the quadrature distribution of the pair coherent state [20]. The two-mode pair cat states exhibit strong nonclassical features due to the correlation between the two modes.

In Fig. 2, we plot the quadratic distribution for different values of the parameter q, (say $q = 2$, 5 and 10). For sufficient small values of the indicator parameter q, the multiparts windows are transformed to a one circular part. This is a consequence of the intrinsic properties of the pair cat state. Nevertheless, perfect purification is not achieved in this case, compared with the case in which small value of ξ is considered (see Figs. 1a and 2a). In Fig. 1a the window is not a two-part function, but is very narrow so that the conditional moment is approximately equal to one circle (this behavior may be obtained if the parameter q takes smaller values). Note that the quadratic distribution is dramatically different from the case when we consider large values of q (see Fig 2a and b, and indeed here it is not possible to observe separate parts of the distribution. It is interesting to see in this figure that the regions of the quadrature distribution in the (x, y)-plane are symmetric with respect to $y = 0$ and also to $x = 0$ (Fig. 2b and c).

In Fig. 3, we set the parameter $\varphi = 0$ and take different values of q and ξ. The evolution of $P(x, y)$ and its responses are similar to that shown in Figs. 1 and 2. It is shown that the regions of the quadrature distribution are symmetric with respect to $x = 0$ and with respect to $y = 0$ (Fig. 3b and c), but the general feature of this case is quite complicated compared with the previous cases. This can be understood from (5), where, when we set $\varphi = 0$ this allows the contribution of the second term in (5). Some of the differences are seen in the contour interval if a very small change of the controller parameters (ξ and q) is considered. This can be demonstrated from a contour plot, such as shown in Fig. 3.

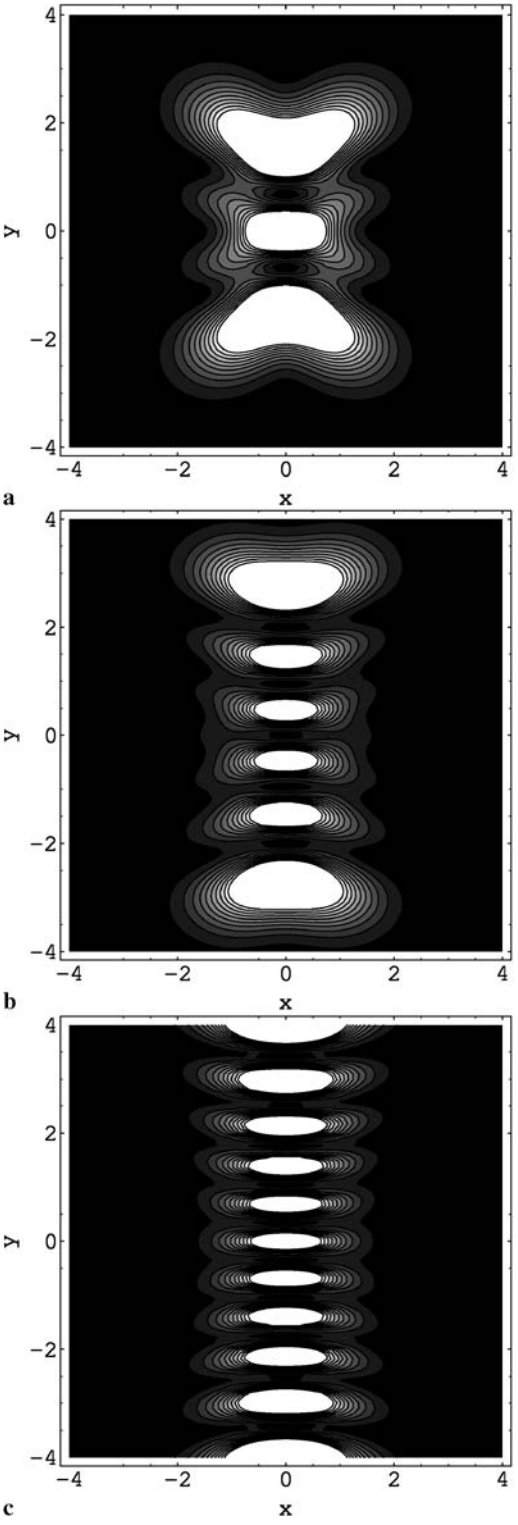

FIGURE 2 Contour plot of the quadrature distribution function $P(x, y)$ for the pair cat state for $\xi = 1$, $\varphi = \pi/2$ and for different values of the parameter q where (**a**) $q = 2$, (**b**) $q = 5$ and (**c**) $q = 10$

3 Physical system and model Hamiltonian

A single trapped ion allows the experimental exploration of the vibrational degrees of freedom and cavity QED [1]. Cirac et al. [21] have shown that the dynamics of a trapped and laser-cooled two-level ion can be described by the JC model. Based on this analogy between trapped ion dynamics and cavity QED, many fascinating proposals [22–24] have been discussed. In this paper, we consider the situation where oscillating classical electromagnetic fields propagating in two-dimensional trap irradiate a single trapped ion. The laser frequency is assumed tuned to the frequency difference between the two modes of the trap. Consequently the Hamiltonian for such a system is given by [1],

$$\hat{H} = \hat{H}_{\mathrm{F}} + \hat{H}_{\mathrm{A}} + \hat{H}_{\mathrm{in}}\,, \tag{8}$$

where

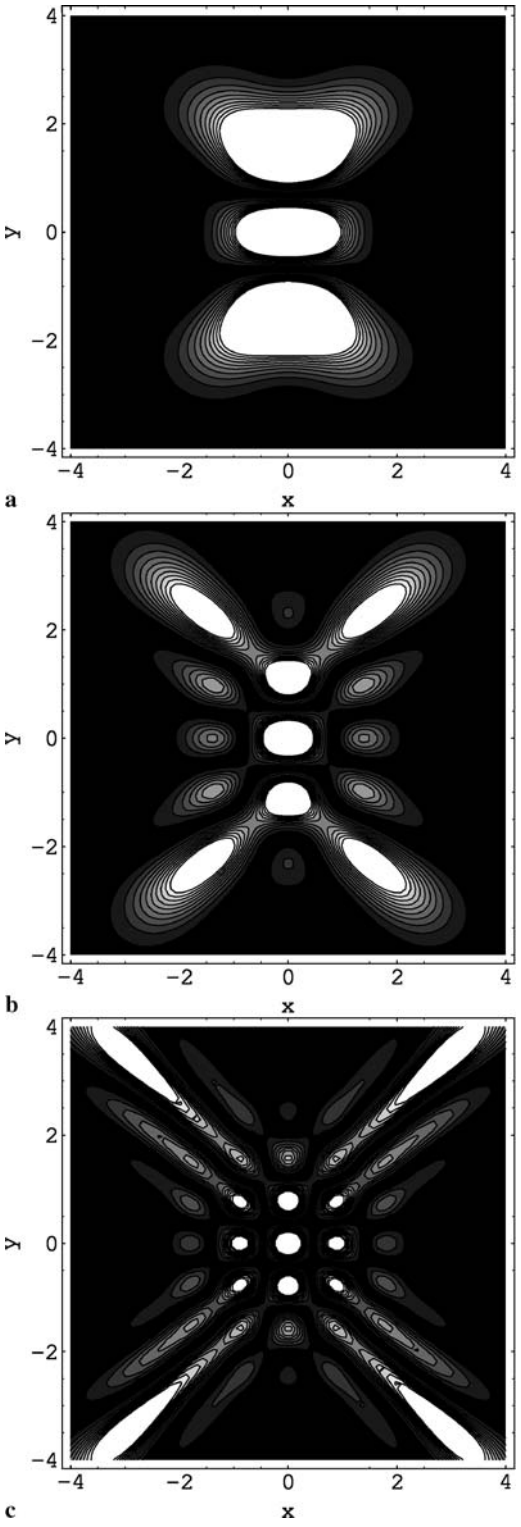

FIGURE 3 Contour plot of the quadrature distribution function $P(x, y)$ for the pair cat state for $q = 2$, $\varphi = 0$ and for different values of the parameter ξ where, (**a**) $\xi = 1$, (**b**) $\xi = 3$ and (**c**) $\xi = 7$

$$\hat{H}_{\rm F} = \hbar\omega_1 \hat{a}_1^{\dagger}\hat{a}_1 + \hbar\omega_2 \hat{a}_2^{\dagger}\hat{a}_2 \,,$$
$$\hat{H}_{\rm A} = \frac{\hbar\omega_0}{2}\hat{\sigma}_z \,,$$
$$\hat{H}_{\rm in} = -\wp.E = -\wp.\varepsilon(vt)[\exp[i(k_1\hat{x} + k_2\hat{y} - \omega t))] + \text{H.c.}] \,,$$

with $\wp$ the dipole matrix element of the ion $\wp = \wp^0(\widehat{\sigma}_+ + \widehat{\sigma}_+)$, $\varepsilon(vt)$ is a modulated amplitude of the irradiating laser field. We denote by ω_i, $(i = 1, 2)$ the fields frequencies, ω_0 the natural frequency of the ion, and v denotes the ionic velocity. Here the $\sigma's$ are the usual 2×2 Pauli matrices satisfying

$$[\hat{\sigma}_z, \hat{\sigma}_\pm] = \pm 2\hat{\sigma}_\pm, [\hat{\sigma}_+, \hat{\sigma}_-] = \hat{\sigma}_z \,. \tag{9}$$

We denote by $\hat{a}_i$ and $\hat{a}_j^{\dagger}$ the Bose operators for the quantized field mode which obey $[\hat{a}_i^{\dagger}, \hat{a}_j] = \Delta_{ij}$, where $\delta_{ij} = 1$ if $i = j$ and **0** otherwise. The operators $\hat{x}$ and $\hat{y}$ are the center of mass position of the ion which are quantized in the forms $\hat{x} = \Delta x(\hat{a}_1^{\dagger} + \hat{a}_1)$, $\hat{y} = \Delta y(\hat{a}_2^{\dagger} + \hat{a}_2)$ and $\Delta x = \sqrt{1/(2v_x M)}$, $\Delta y = \sqrt{1/(2v_y M)}$ with M being the mass of the trapped ion.

Making use of the special form of Baker–Hausdorff theorem [25] the operator $\exp[i\eta(\hat{a}^{\dagger} + \hat{a})]$ may be written as a product of operators i.e.,

$$\begin{aligned} \mathrm{e}^{i\eta(\hat{a}^{\dagger}+\hat{a})} &= \exp\left(\frac{\eta^2}{2}[\hat{a}^{\dagger}, \hat{a}]\right)\exp\left(i\eta\hat{a}^{\dagger}\right)\exp\left(i\eta\hat{a}\right) \\ &= \mathrm{e}^{-\eta^2/2}\sum_{n=0}^{\infty}\frac{(i\eta)^n\,\hat{a}^{\dagger n}}{n!}\sum_{m=0}^{\infty}\frac{(i\eta)^m\,\hat{a}^m}{m!} \,. \end{aligned} \tag{10}$$

Using (10), the interaction part of (8) can be written as

$$\begin{aligned} \hat{H}_{in} = &-\wp^0.\varepsilon(vt)\eta_1\eta_2\exp\left[-\frac{1}{2}(\eta_1^2 + \eta_2^2)\right] \\ &\times\sum_{l=0}^{\infty}\sum_{m=0}^{\infty}\frac{\hat{a}_1^{\dagger l}\hat{a}_1^l\hat{a}_2^{\dagger m}\hat{a}_2^m}{(l+1)!(m+1)!}(i\eta_1)^l(i\eta_2)^m \\ &\times\left(\hat{a}_1^{\dagger}\hat{a}_2 + \hat{a}_2^{\dagger}\hat{a}_1\right)(\hat{\sigma}_- + \hat{\sigma}_+) \,, \end{aligned} \tag{11}$$

with $\eta_1 = k_1\Delta x$ and $\eta_2 = k_2\Delta y$. In the Lamb–Dicke limit and within the rotating wave approximation then the effective interaction Hamiltonian (11) takes the two photon bimodal interaction form. However, provided we adjust the strength of the electric field to include the time dependent factor $\varepsilon(vt)$.

In the Lamb–Dicke regime, $\eta_j \ll 1$, (11), can be well approximated by expanding the exponential terms up to second order in η $(\eta = \eta_1 = \eta_2)$,

$$\hat{H}_{in} = \hbar\lambda(t)\hat{a}_1^{\dagger}\hat{a}_2\hat{\sigma}_- + \text{H.c} \,, \tag{12}$$

where $\lambda(t) = -\varepsilon(vt)\wp^0\eta^2\exp\left(-\frac{\eta^2}{2}\right)$.

The equations of motion for the operators $\hat{a}_i(t)$, $\hat{\sigma}_\pm(t)$ and $\hat{\sigma}_z(t)$ in the Heisenberg picture according to the Hamiltonian (8) are

$$\begin{aligned} \frac{\mathrm{d}\hat{a}_1}{\mathrm{d}t} &= -i\omega_1\hat{a}_1 - i\lambda(t)\hat{a}_2\hat{\sigma}_- \,, \\ \frac{\mathrm{d}\hat{a}_2}{\mathrm{d}t} &= -i\omega_2\hat{a}_2 - i\lambda(t)\hat{a}_1\hat{\sigma}_+ \\ \frac{\mathrm{d}\sigma_-}{\mathrm{d}t} &= -i\omega_0\sigma_- + i\lambda(t)\hat{a}_1\hat{a}_2^{\dagger}\sigma_z \,, \\ \frac{\mathrm{d}\sigma_z}{\mathrm{d}t} &= 2i\lambda(t)\left(\hat{a}_1^{\dagger}\hat{a}_2\hat{\sigma}_- - \hat{a}_1\hat{a}_2^{\dagger}\hat{\sigma}_+\right) \,. \end{aligned} \tag{13}$$

After straightforward calculations, one can find an analytic time dependent solution as

$$\hat{a}_1(t) = e^{i\hat{\mu}\alpha(t)}\left(\cos(\gamma_1\alpha(t)) - \frac{i\hat{\mu}}{\gamma_1}\sin(\gamma_1\alpha(t))\right)\hat{a}_1(0) - \frac{i}{\gamma_1}e^{-i\omega_1 t}e^{i\hat{\mu}I(t)}\sin(\gamma_1\alpha(t))\hat{a}_2(0)\hat{\sigma}_-(0), \quad (14)$$

$$\hat{a}_2(t) = e^{-i\omega_2 t}e^{i\hat{\mu}\alpha(t)}\left(\cos(\gamma_2\alpha(t)) - \frac{i\hat{\mu}}{\gamma_2}\sin(\gamma_2\alpha(t))\right)\hat{a}_2(0) - \frac{i}{\gamma_2}e^{-i\omega_2 t}e^{i\hat{\mu}\alpha(t)}\sin(\gamma_2\alpha(t))\hat{a}_1(0)\hat{\sigma}_+(0), \quad (15)$$

$$\hat{\sigma}_-(t) = -\frac{i}{\gamma_3}e^{-i\omega_{12}t}e^{i\hat{\mu}\alpha(t)}\sin(\gamma_3\alpha(t))\hat{a}_1(0)\hat{a}_2^\dagger(0) + e^{-i\omega_{12}t}e^{i\hat{\mu}\alpha(t)}\left(\cos(\gamma_3\alpha(t)) + \frac{i\hat{\mu}}{\gamma_3}\sin(\gamma_3\alpha(t))\right)\hat{\sigma}_-(0)\,, \quad (16)$$

$$\hat{\sigma}_z(t) = \cos(2\gamma_4\alpha(t))\hat{\sigma}_z(0) + \frac{i}{\gamma_4}\sin(2\gamma_4\alpha(t)) \times \left(\hat{a}_2^\dagger\hat{a}_1\hat{\sigma}_+(0) - \hat{a}_1^\dagger\hat{a}_2\hat{\sigma}_-(0)\right)\,, \quad (17)$$

where $\omega_{12} = \omega_1 - \omega_2$,

$$\gamma_1 = \left(\hat{l}+\frac{1}{2}\right)\left(\hat{m}+\frac{3}{2}\right),\ \gamma_2 = \left(\hat{l}+\frac{3}{2}\right)\left(\hat{m}+\frac{1}{2}\right),$$
$$\gamma_3 = \left(\hat{l}-\frac{1}{2}\right)\left(\hat{m}+\frac{3}{2}\right),\ \gamma_4 = \left(\hat{l}+\frac{1}{2}\right)\left(\hat{m}+\frac{1}{2}\right),$$
$$\alpha(t) = \int_0^t \lambda\left(t'\right)\mathrm{d}t',\ \hat{\mu} = \left(\hat{a}_1^\dagger\hat{a}_2\hat{\sigma}_- + \hat{a}_2^\dagger\hat{a}_1\hat{\sigma}_+\right).$$

Having obtained the dynamical operators, we now discuss some statistical properties of the system.

4 Atomic inversion

The entanglement of motional degrees of freedom of the center of mass of the ion with its internal degrees of freedom manifests itself in the well known collapse and revival of population inversion [26]. The (internal level) ionic dynamics depend on the distributions of initial excitations of both the field and the center-of-mass vibrational motion, given by $\langle n|\varrho_{\mathrm{f}}(0)|n\rangle = \varrho^f_{nn}(0)$ and $\langle m|\varrho_{\mathrm{v}}(0)|m\rangle = \varrho^v_{mm}(0)$, respectively. For instance, the atomic population inversion may be written as

$$\langle\sigma_z(t)\rangle = Tr\left(\sigma_z(0)\varrho(t)\right)\,. \quad (18)$$

that is the difference between the probability of finding the system in the ground state and the probability of finding the system in the excited state.

To analyze the effects resulting from variation in the parameter $\lambda(t)$ on the atomic inversion we have plotted in Fig. 4 the function $\langle\sigma_z(t)\rangle$ against the scaled time λt, for different values $\lambda(t)$, where $\lambda(t) = \lambda$ for Fig. 4a and $\lambda(t) = \lambda\sinh(\varpi t)$ for Fig. 4b, where ϖ is a positive integer. In this figure we take the parameters $\xi = 10$, $q = 1$ and $\varphi = \pi/2$, at exact resonances. In Fig. 4a we find that the value of the atomic inversion decreases to its minimum, (approximately -0.75) then it

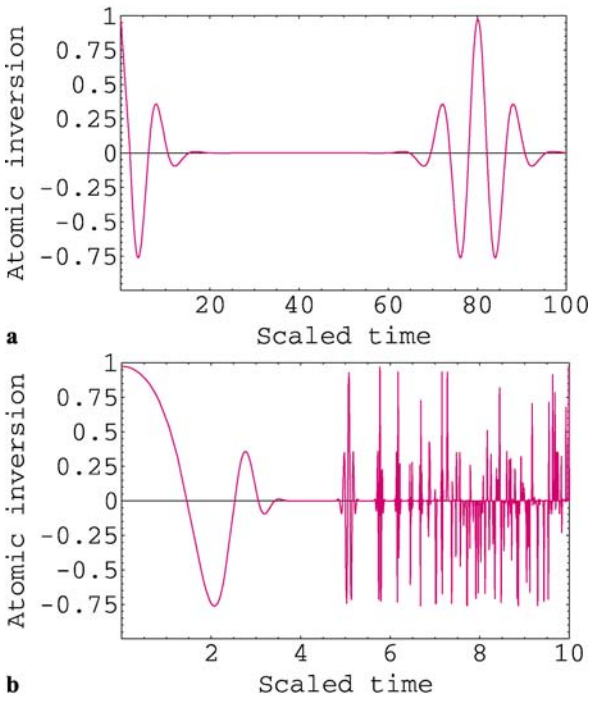

FIGURE 4 The atomic inversion as a function of the scaled time λt. Parameters: $\xi = 10$, $q = 1$, $\varphi = 0$, where (**a**) $\lambda(t) = \lambda t$ and (**b**) $\lambda(t) = \lambda\sinh(\varpi t)$

collapses and starts to fluctuate around zero for a short period of time. Thus the Rabi frequencies become commensurate so that the atomic inversion has an exact periodic evolution with a scaled λ-dependent period. In this case there are no oscillations in the collapse region, as shown in Fig. 4a. A different pattern for the oscillations occurs if the number difference is slightly changed. Strictly speaking, when we consider the time dependent modulating function $\lambda(t) = \lambda\sinh(\varpi t)$. The appearance of the collapses and revivals in almost a periodic way has been washed out in this case. On the other hand and in the presence of the time-dependent modulating function we find the behavior of the atomic inversion function is drastically changed where we see irregular collapses and revivals occur, (see Fig. 4b). The short time revivals are strongly suppressed, as we see in Fig. 4b. We may compare the atomic inversion in both Figs. 3a and Fig. 3b, in the former case the collapse time is long enough to allow for revivals, while in the latter a shorter collapse time with the same amplitudes of the revivals.

It is interesting to explore to what conditions can be considered to generate a long living entanglement. This will be seen in the next section.

5 Entanglement

Entanglement between several particles is an important feature of many quantum communication and computation protocols. To see how the entanglement of ion–field interaction is affected by the presence of pair cat states for the aforementioned system we start from a factored initial state of both the ion and field. We consider the notion of entanglement entropy, that is, considering a quantum system in a pure state with the density matrix of the remaining space as $\varrho_A = Tr_F\left(\varrho\right)$. The density matrix contains all information of

any system in a mixed or pure state, and computing vital physical information on any such system is mostly determined by the eigenvalues of the density matrix. The partial entropy of entanglement for a bipartite pure state is defined as Von Neumann entropy of the reduced state,

$$S_{\mathrm{A}} = -Tr\left\{\varrho_{\mathrm{A}} \ln \varrho_{\mathrm{A}}\right\} . \tag{19}$$

This procedure is well established, and works well for all cases where the initial state of the system is in a pure state. Most work has been focused on this entanglement in time-independent modulating function. Here we consider the time-dependent case.

On the other hand, the quantum entropy of the field $S_{\mathrm{f}}(t)$ can be expressed in terms of the eigenvalues $\lambda_{\mathrm{F}}^{\pm}(t)$ of the reduced field density operator as follows

$$S_{\mathrm{f}}(t) = -[\lambda_{\mathrm{f}}^{+}(t) \ln \lambda_{\mathrm{f}}^{+}(t) + \lambda_{\mathrm{f}}^{-}(t) \ln \lambda_{\mathrm{f}}^{-}(t)] . \tag{20}$$

In the case of a disentangled pure joint state $S_{\mathrm{f}}(t)$ is zero, and for maximally entangled states it gives $\ln 2$ [9–11]. Due to the higher dimensionality of the problem we cannot obtain a simple analytical expression for (20), therefore the numerical approach becomes indispensable.

First, we consider the behavior of the field entropy in the case of the time-independent modulating function $\lambda(t) = \lambda$ (constant). Figure 5 is a plot of quantum field entropy $S_{\mathrm{f}}(t)$ as a function of scaled time parameter λt for $\eta = 0.2$ and different values of ξ where $\xi = 10$ for Fig. 5a and $\xi = 20$ for Fig. 5b. Our numerical analysis was performed using other parameters from [14, 24], where a trapped $^{9}Be^{+}$ ion was laser-cooled to the zero-point of motion.

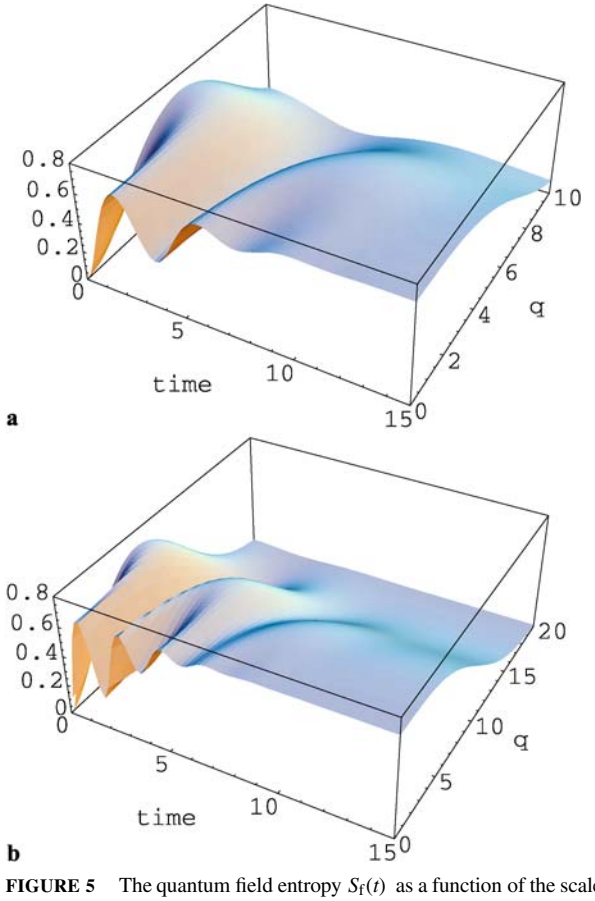

FIGURE 5 The quantum field entropy $S_{\mathrm{f}}(t)$ as a function of the scaled time λt. The parameters are $q = 1$, $\eta = 0.2$, $\lambda(t) = \lambda$ and different values of ξ where (**a**) $\xi = 10$ and (**b**) $\xi = 20$

It is interesting to note that, the maximum entanglement decreases as the parameter q increased (see Fig. 5a). As time goes on we note a growth in $S_{\mathrm{f}}(t)$, followed by a sudden decrease, almost down to zero at large values of q. A further increase in time and for smaller values of q makes the entanglement survives longer. The constat value of $S_{\mathrm{f}}(t)$ is interpreted as a result of quantum entanglement between ion and fields, surviving for a long time interaction. However, an interesting situation may arise when the parameter ξ takes large values (say 20 in Fig. 5b). In this case, for some small fixed values of q, the entanglement surviving starts at earlier time with the number of oscillations increased with increasing ξ. Also, the amplitudes of these oscillations are bigger compared to the case in which $\xi = 10$ (see Fig. 5a and b). As seen in the entropy plot in Fig. 5b, the pure state is basically obtained for large values of the parameter q (because the natural scale of q is between 0 and ξ, in Fig. 5b, we expand the scale of q to take values between 0 and 20).

On the contrary, as can be seen from Fig. 5, if the fields are initially prepared in a pair cat state and the modulating function is taken to be time-dependent $\lambda(t) = \lambda \sinh(\varpi t)$, then the entanglement parameter is significantly larger than zero for any time $t > 0$, but with occasional oscillations. Also, the number of oscillations is increased as the parameter q decreases associated with low entanglement reaches zero for smaller values of the parameter ξ (see Fig. 6).

Another interesting aspect is that the time-dependent modulating function $\lambda(t)$ has an important effect on the entanglement, where, the total ion–field state can not have its purity diminished, which means that as the field becomes more pure the ionic state must be closer to a mixed state. Also, in this case, it seems remarkable that entanglement survives for long-time with some oscillations. Hence, for a time-independent modulating function, we would expect entanglement to survive longer.

Practically speaking, as can be deduced from Fig. 5a, the oscillations in the entanglement between the ion and the field quickly damp out with an increase in q. The subsystem will not disentangle from each other until the steady state is reached as long as the interaction is present. This means that neither the ion nor the field will return back to a pure state except at the beginning of the interaction and $t \to \infty$, contrast to the $q = 0$ case. In order to gain insight into the general behavior we have considered different values of ξ in Fig. 6b where we notice that the amplitude of the oscillations in the entanglement is increased with increasing ξ.

The remaining task is to identify and compare the results presented above for the entanglement degree with another accepted entanglement measure such as the linear entropy. The question of the ordering of entanglement measures was raised in [28]. It was proved that all good asymptotic entanglement measures are either identical or fail to uniformly give consistent orderings of density matrices [33]. In order to better characterize the subsystems, we may refer here to another measure of the entanglement of a reduced density matrix which is the

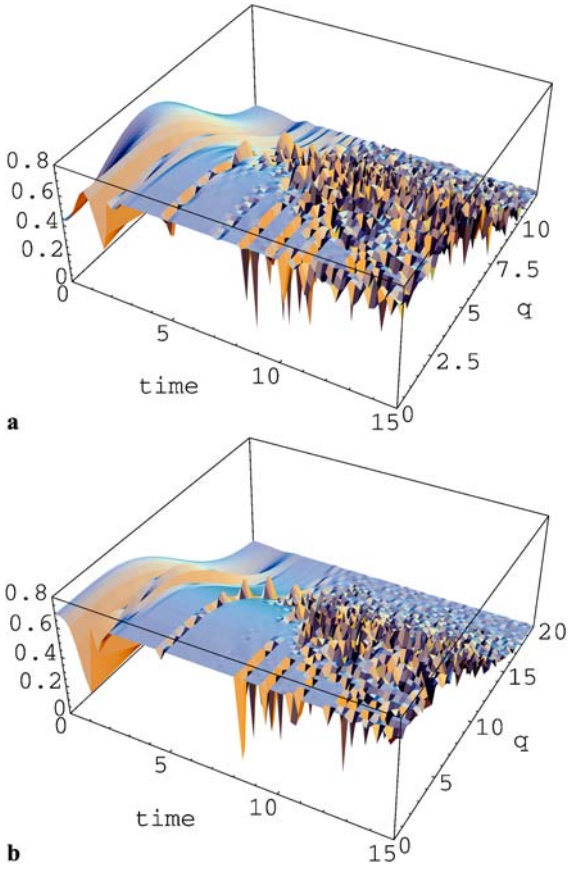

FIGURE 6 The same as Fig. 5 but $\lambda(t) = \lambda \sinh(\varpi t)$

product state identification

$$S_{\mathrm{L}} = 1 - Tr\varrho_{\mathrm{A}}^{n}, \qquad n \geq 2\,, \tag{21}$$

which is zero for a product state, and unity for a maximally entangled state. This measure is equivalent to the Rĕnyi entropy [29–32] and is not well suited for much more than to single out a pure state, as with increasing n any entangled state will converge to zero in this measure.

In Fig. 7 we plot the entanglement according to a high order linear entropy as compared with the von Neumann entropy. One, possibly not very surprising, principal observation is that the numerical calculations corresponding to the same parameters, which have been considered in Figs. 4 and 5, gives nearly the same behavior (see Fig. 7). This means that both the entanglement due to the quantum field entropy S_{f} and high order linear entropy S_{L} measures are qualitatively the same. The important consequence of this observation is that the use of quantum entropy and linear entropy as measures of entanglement are equivalent. We must stress, however, that no single measure alone is enough to quantify the entanglement in a multi-partite systems. Finally, we may say that, it is possible to obtain a long living entanglement using the time-independent modulating function in a pair cat state. This result is quite surprising, since the previous studies [9–11] in the entanglement for the time-independent interaction for the initial coherent state does not contain this interesting feature. Which means that the pair cat state as an initial state of the field plays very important roles in obtaining long-lived entanglement.

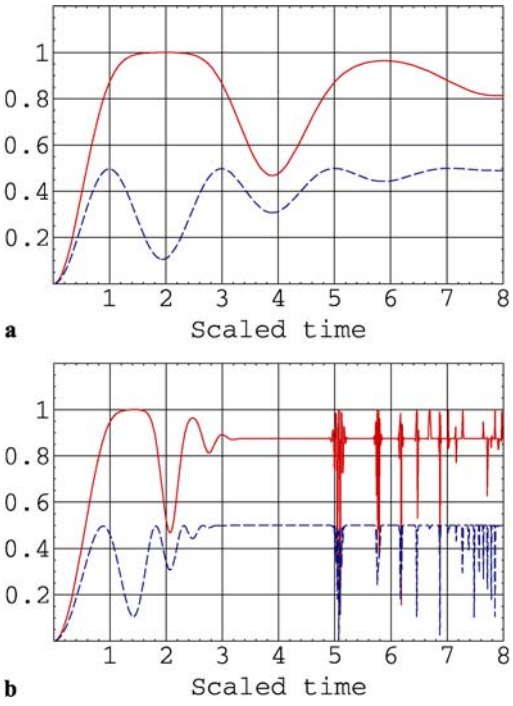

FIGURE 7 Time evolution of entanglement degree S_{L} as a function of the scaled time λt. The parameters are the same as in Fig. 5, where $n = 2$ (the *solid curve*) and $n = 3$ (the *dotted curve*)

A proposal for the generation of motional pair cat states in a two-dimensional anisotropic trap has been given in [34]. In order to generate the pair cat states for the motion in a two-dimensional anisotropic trap we require two laser beams and the frequencies of the laser beams are chosen as $\omega_1 = \omega_0 - 2\nu_x - 2\nu_y$, and $\omega_2 = \omega_0$. Apart from detecting quantum entanglement in these states, it might be a useful way to fully characterize simple quantum logic gates [35].

6 Summary

We have considered the problem of the interaction between a single trapped ion and laser fields. We have shown that the input pair cat states exhibit strong nonclassical features due to the correlation between the two modes. The phenomenon of quantum revivals in the time-dependent ion–field interaction and the atomic inversion properties as well as the entanglement have been analyzed. Also, it has been shown that the atomic inversion as a function of the scaled time may display different structures of beats depending on the initial state of the field and the vibrational motion as well as on the time-dependent interaction. Effects such as suppression or attenuation of the Rabi oscillations and long time scale revivals as well as aperiodic dynamics have been observed.

Using pair cat states as an initial state of the fields, we have analytically shown that the fluctuations of the entanglement between maximum and minimum values are irregular for both the time-independent and time-dependent cases at a short period of the interaction time. Our results reveal a new feature in the entanglement as a function of the scaled time, that is a long living entanglement. This feature depends on the parameters ξ and q. These interesting features may pave the way to quantum information applications such as deter-

ministic all-optical quantum computation. The results can be relevant for basic studies on entanglement as well as for applications in the preparation and manipulation of quantum states for quantum information purposes. As far as scalability is concerned, one could think in having several trapped ions in a high-Q cavity, exchanging information via the cavity photons, or other more sophisticated schemes involving trapped ions, phonons and photons.

It is to be remarked that, the entropy of entanglement can be determined indirectly by experiment using the quantum state tomography [4, 5]. This fact comes from the definition of the entropy of entanglement which is associated with the density matrix of quantum state. We believe that the pair cat states may be a useful tool to be considered in obtaining a long living entanglement of systems of indistinguishable particles. While our analysis was carried out with respect to the example of a single trapped ion beyond Lamb–Dicke regime, we emphasize that the results reported here apply equally well to any bipartite system. We hope to report on such issues in a forthcoming paper.

ACKNOWLEDGEMENTS The author would like to thank the referees for their objective comments that improved the text in many points. Also, it is a pleasure to thank G. Gour, A.-S.F. Obada, S.S. Hassan, and M.S. Abdalla for inspiring discussions.

REFERENCES

1 For an overview of theoretical and experimental work on quantum dynamics of single trapped ions, see, for example, D. Leibfried, R. Blatt, C. Monroe, D. Wineland, Rev. Mod. Phys. **75**, 281 (2003)
2 C. Monroe, D.M. Meekhof, B.E. King, S.R. Jeffers, W.M. Itano, D.J. Wineland, P. Gould, Phys. Rev. Lett. **75**, 4011 (1995)
3 C. Monroe, D.M. Meekhof, B.E. King, D. Leibfried, W.M. Itano, D.J. Wineland, Acc. Chem. Res. **29**, 585 (1996)
4 D. Leibfried, D.M. Meekhof, B.E. King, C. Monroe, W.M. Itano, D.J. Wineland, Phys. Rev. Lett. **77**, 4281 (1996)
5 J.F. Poyatos, R. Walser, J.I. Cirac, R. Blatt, P. Zoller, Phys. Rev. A **53**, R1966 (1996)
6 D. Leibfried, D.M. Meekhof, B.E. King, C. Monroe, W.M. Itano, D.J. Wineland, J. Mod. Opt. **44**, 2485 (1997)
7 C.H. Bennett, H.J. Bernstein, S. Popesu, B. Schumacher, Phys. Rev. A **53**, 2046 (1996)
8 V. Vedral, M.B. Plenio, K. Jacobs, P.L. Knight, Phys. Rev. A **56**, 4452 (1997)
9 S.J.D. Phoenix, P.L. Knight, Ann. Phys. (New York) **186**, 381 (1988)
10 S.J.D. Phoenix, P.L. Knight, Phys. Rev. A **44**, 6023 (1991)
11 S.J.D. Phoenix, P.L. Knight, Phys. Rev. Lett. **66**, 2833 (1991)
12 C. Becher, J. Benhelm, D. Chek-Al-Kar, M. Chwalla, H. Häffner, W. Hänsel, T. Körber, A. Kreuter, G.P.T. Lancaster, T. Monz, E.S. Phillips, U.D. Rapol, M. Riebe, C.F. Roos, C. Russo, F. Schmidt-Kaler, R. Blatt, *Laser Spectroscopy*, ed. by E.A. Hinds, A. Ferguson, E. Riis (World Scientific, 2005), pp. 381–392
13 E. Schrödinger, Naturwissenschaften **48**, 807 (1935)
14 C. Monroe, D.M. Meekhof, B.E. King, D.J. Wineland, Science **272**, 1131 (1996)
15 V. Bužek, A. Vidiella-Barranco, P.L. Knight, Phys. Rev. A **45**, 6570 (1992)
16 J.R. Klauder, B. Skagerstam, *Coherent States: Applications in Physics and Mathematical Physics* (World Scientific, Singaporem, 1985)
17 G.S. Agarwal, J. Opt. Soc. Am. B **5**, 1940 (1988)
18 G.S. Agarwal, Phys. Rev. Lett. **57**, 827 (1986)
19 C.C. Gerry, R. Grobe, Phys. Rev. A **51**, 1698 (1995)
20 G.S. Agarwal, A. Biswas, G.S. Agarwal, J. Opt. B Quantum Semiclass. Opt. **7**, 350 (2005)
21 J.I. Cirac, R. Blatt, A.S. Parkins, P. Zoller, Phys. Rev. Lett. **70**, 762 (1993)
22 J.I. Cirac, R. Blatt, A.S. Parkins, P. Zoller, Phys. Rev. A **49**, 1202 (1994)
23 I. Marzoli, J.I. Cirac, R. Blatt, P. Zoller, Phys. Rev. A **49**, 2771 (1994)
24 D.M. Meekhof, C. Monroe, B.E. King, W.M. Itano, D.J. Wineland, Phys. Rev. Lett. **76**, 1796 (1996)
25 C.A. Blockley, D.F. Walls, H. Risken, Europhys. Lett. **17**, 509 (1992)
26 S.S. Sharma, N.K. Sharma, J. Phys. B **35**, 1643 (2002)
27 A.B. Mundt, A. Kreuter, C. Becher, D. Liebfried, J. Eschner, F. Schmidt-Kaler, R. Blatt, Phys. Rev. Lett. **89**, 103 001 (2002)
28 J. Eisert, M.B. Plenio, J. Mod. Opt. **46**, 145 (1999)
29 S.O. Skroseth, K. Olaussen, Phys. Rev. A**72**, 022 318 (2005)
30 B.-Q. Jin, V.E. Korepin, J. Statist. Phys. **116**, 79 (2004)
31 S.O. Skrvseth, arXiv:quant-ph/0508160 (2005)
32 M. Ziman, V. Buzek, Phys. Rev. A **73**, 012 312 (2006)
33 S. Virmani, M.B. Plenio, Phys. Lett. A **268**, 31 (2000)
34 S.-B. Zheng, J. Opt. B Quantum Semiclass. Opt. **3**, 298 (2001)
35 J.F. Poyatos, J.I. Cirac, P. Zoller, Phys. Rev. Lett. **78**, 390 (1997)